

Sample size effect in coercivity measurement of epitaxial magnetic garnet films

G. Vértesy and M. Pardavi-Horváth

Central Research Institute for Physics, Hungarian Academy of Sciences, H-1525 Budapest, P.O. Box 49, Hungary

I. Tomáš and L. Půst

Institute of Physics, Czechoslovak Academy of Sciences, 180 40 Prague 8, Na Slovance 2, Czechoslovakia

(Received 10 April 1987; accepted for publication 1 October 1987)

The full set of characteristic parameters of epitaxial garnet films was measured as a function of the sample size from about 2000 to 5 mm². The type of domain structure, width of the stripe domain period, characteristic material length, domain wall energy, and anisotropy did not change within the error of measurement on reducing the sample size. The bubble domain collapse field decreased by about 2.5%, and the domain wall coercivity was measured and found to have decreased—almost by an order of magnitude. The experiments showed the lack of dependence of coercivity on the domain wall length. The coercivity and collapse field are suggested as being related to the sample dimensions via the sample-size-dependent derivatives of the total free energy with respect to the domain wall positions. The assumption of the direct effect of the free energy derivatives on the coercivity is supported by a model experiment.

I. INTRODUCTION

Single crystalline magnetic garnet layers grown by the liquid-phase epitaxy method on nonmagnetic garnet substrates were developed for bubble memory devices in the early 1970s. Crystals of (YSmCa)₃(FeGe)₅O₁₂ with a domain size of 1–5 μm are the most typical materials. Because of their very high quality, simple stripe and bubble domain structure, and simple magnetization process by means of domain wall displacement, these garnets represent very good model materials for investigating fundamental questions of magnetization processes.

In bubble memory applications the characterization of samples is performed on wafers of 5 or 7.5 cm diam, and following microelectronic processing, the wafers are cut into chips of about 1 cm². Parallel samples for research purposes are cut from large pieces, too, and usually it is tacitly assumed that none of the material parameters change on cutting the sample.

However, some shift of parameters has been observed experimentally. In this paper a systematic investigation of the wafer cutting effects on the magnetic parameters of the crystals is reported. A drastic decrease of coercivity with decreasing sample size has been observed, and the origin of this effect has been analyzed.

II. EXPERIMENTS

Epitaxial garnet films of the well-known common bubble material (YSmCa)₃(FeGe)₅O₁₂ were chosen for the investigation. Films were grown by liquid-phase epitaxy (LPE) on (111)-oriented 5-cm-diam Gd₃Ga₅O₁₂ (GGG) substrates. Film properties, measured by standard methods of bubble film characterization, were typical of 5-μm bubble material, except for the coercivity H_c , which was extremely high for one of the two crystals (sample A, $H_c = 3.3$ Oe) chosen as representative samples in this paper.

The garnet film on the back of the substrate was removed by mechanical polishing prior to the measurements. The characteristic parameters were measured at many points on the wafer before dicing, and after cutting, the measurements were repeated at the same points. The dicing was carried out in consecutive steps, to obtain smaller and smaller samples, and all the parameters were remeasured after each step. The sample size was decreased from 2000 to 5 mm².

The static coercivity H_c was measured by using the low-frequency (200-Hz) domain wall oscillation method¹; that is, the amplitude of an ac field, oriented perpendicular to the sample plane, was increased linearly from zero, and the response of the moving domain walls was detected photoelectrically. The measurement was performed on stripes (in zero external bias field) and on bubble domains by the same method in the presence of a static bias field H_b ($H_{\text{stripe out}} < H_b < H_0$, H_0 being the bubble collapse field). Bubbles were generated by field pulses, which cut the stripes, and then—by increasing the bias field—a bubble lattice was created from the short stripes. The same value of H_b was used in every measurement for a given sample. On large (250-mm²) pieces of both samples, the bias field dependence of the bubble domain coercivity was measured, too, i.e., the dependence of coercivity on bubble domain size.

The coercivity of stripe domains was measured for different stripe patterns and/or domain length on large (250-mm²) samples, i.e., for stripe domains obtained by demagnetization in a decreasing normal ac field and for domain patterns obtained by application of field pulses. In the former case, shown in Fig. 1, the domains are long, and they expand from one edge of the sample to the other; in the latter case (Fig. 2) the original long stripes are cut into small segments of length of about 50–200 μm.

Most of the coercivity measurements were performed in

a polarizing microscope, where magnetic field coils and a photodetector are built into the microscope. The outside and inside diameter of the ac-field coil are 25 and 10 mm, respectively. The stripe domain coercivity versus sample size measurement was repeated in another apparatus, built on an optical bench with a He-Ne laser as the polarized light source. The apparatus did not contain any optical element apart from an analyzer, and a large coil (inside diameter 35 mm) produced the ac field. If a small-diameter ac-field coil is used, the measurement area of the oscillating domains is situated in a sea of stationary domains, whereas if the measurement is performed with the large coil, the domain walls move in the whole sample (except for the largest samples). A third variation, i.e., moving domain walls in a sea of saturated sample, was also realized, by using a small- and large-diameter bias coil producing opposite magnetic fields, the sum of the fields being equal to zero in the actual measurement area.

The collapse field H_0 of the bubble domains was measured by an increasing-amplitude ac-field method.² Bubbles subjected to static bias field H_b were acted upon by a low-frequency (200-Hz) ac field with slowly increasing amplitude. The photoelectrically detected response of the "breathing" domains showed a sudden breakdown at the amplitude when the bubbles collapse. In another series of measurements, an additional constant-amplitude high-frequency field (10 Oe, 10 kHz) was present during the whole measurement series. All the fields were oriented normal to the sample surface.

The stripe domain period p_0 and the effective anisotropy field H_k^{eff} were measured as a function of sample size by methods described in Refs. 3 and 4. The values of p_0 and H_0 were determined as a function of the distance from the sample edge. Otherwise, all the parameters were measured in the center of the samples. The surface roughness was measured by a Talystep surface profiler with better than 1-nm sensitivity. The accuracy of H_c , H_0 , p_0 , and H_k^{eff} measurements was ± 0.1 Oe, ± 1 Oe, $\pm 0.1 \mu\text{m}$, and ± 10 Oe, respectively. All measurements were performed at room temperature.

III. RESULTS

The most important parameters of the investigated samples are summarized in Table I.

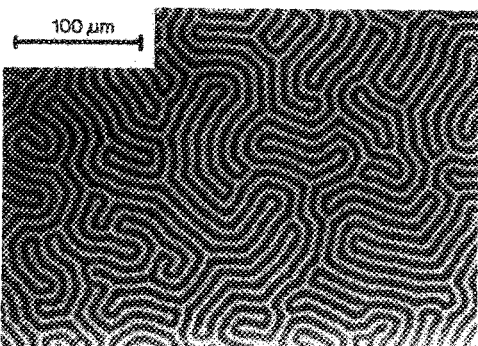


FIG. 1. Stripe domain structure of a garnet film, demagnetized by decreasing ac field, applied normal to sample surface.

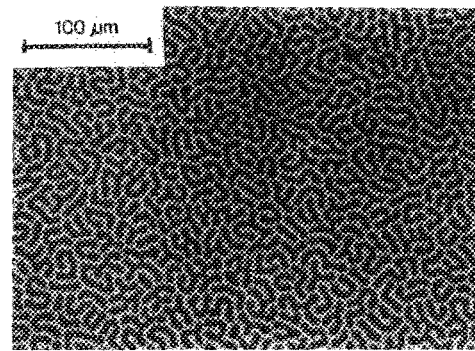


FIG. 2. Stripe domain structure after application of field pulses normal to surface.

The dependence of the coercivity on the sample size can be seen in Figs. 3 and 4 for the two crystals of Table I. H_c^s denotes the coercivity measured on stripes, and H_c^b is the coercivity measured on bubble domains. It is seen that the stripe domain coercivity decreases by one order of magnitude for sample A with decreasing sample size. These figures illustrate the results of measurements made in the microscope with the small-diameter ac-field coils. The measurement series performed in the laser equipment with the large coil provided the same value for the coercivity and the same size dependence. Similarly, when the field distribution was changed, i.e., when the sample was saturated around the measured area, it had no effect on the value or on the size dependence of the coercivity.

The bubble domain coercivity H_c^b also decreases with sample size, but not as rapidly as H_c^s , and it starts to change at smaller sample size. The measurements were performed on a bubble lattice, where the average distance between the centers of bubbles was about $35 \mu\text{m}$, i.e., about seven bubble diameters. The density of the bubbles did not change when the sample size was reduced.

Figure 5 shows the behavior of the bubble collapse field with decreasing sample size. There is a definite decrease of H_0 about 2.5%, but it becomes pronounced only below about $S \approx 1 \text{ cm}^2$.

The stripe domain period and effective anisotropy field do not depend on sample size. The character of the domain structure did not change with sample size.

The effect of sample edge on the stripe domain period and collapse field can be seen in Figs. 6(a) and 6(b), where p_0 and H_0 are given as a function of distance x measured from the edge of the sample. Very near to the sample edge, p_0 and H_0 are reduced, the stripe period reaches the value that was measured at the center of the sample at a distance of about $6p_0$ ($\approx 60 \mu\text{m}$) from the edge, and the collapse field does the same at a distance of about $40p_0$ from the edge.

As shown in Table II, there was no measurable difference in the coercivity of the different stripe domain patterns of Figs. 1 and 2, and similarly, the H_c^b coercivity was the same for bubbles of different domain diameter, as illustrated in Fig. 7. The stripe domain coercivity of the smallest samples was not influenced if a large piece of sample was brought into mechanical contact with the small sample. Application

TABLE I. Magnetic properties of 5-cm-diam epitaxial garnet wafers ($4\pi M_s$, saturation magnetization; H_c , stripe domain coercivity; K_u , uniaxial anisotropy constant; h , thickness; H_0 , bubble collapse field; p_0 , stripe domain period; $\delta_0 = \sqrt{A/K_u}$, domain wall width; $\gamma_w = 4\sqrt{AK_u}$, domain wall energy; l , characteristic material length).

Sample	$4\pi M_s$ (G)	H_c (Oe)	K_u (erg cm ⁻³)	h (μm)	H_0 (Oe)	p_0 (μm)	δ_0 (μm)	γ_w (erg cm ⁻¹)	l/h
A	211	0.5	9040	5.3	120.5	9.0	0.048	0.17	0.087
B	205	3.3	8880	5.4	105.5	10.5	0.047	0.17	0.114

of the 10-kHz frequency and 10-Oe amplitude ac field during the collapse field measurement caused a slight change in the absolute value of the collapse field, but the size dependence remained unchanged. No difference in the surface roughness was experienced for different size samples.

IV. DISCUSSION

In an endeavor to understand the dependence of the measured coercivity on sample size, we considered the existing theories of coercivity as well as the details of the method of measurement.¹

A. Domain-wall-length dependence

In the case of stripe domains, one may assume that in larger samples the stripe domains are longer, because the stripes tend to be as long as possible. In such a way the domain length could be scaled by the sample size. There are several models of coercivity⁵⁻⁸ in which the domain wall length is involved, and a connection between coercivity and domain wall length is expressed. By using these models the coercivity could be related to the sample size and, in such a way, compared with our experiments. On samples of unchanged size, however, no coercivity dependence on the domain wall length was observed. The coercivity H_c^s , measured on any sample of a fixed size, had the same value no matter how long the stripe domains were (see Table II, which compares measurements on stripes of Figs. 1 and 2), and also, H_c^b measured on bubbles was the same no matter how large the bubbles were, provided they were sufficiently well separated from each other (see Fig. 7). Judging from our measurements, the coercivity does not depend on the domain wall length.

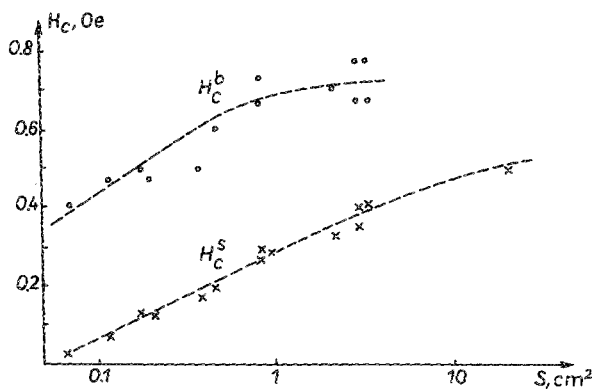


FIG. 3. Dependence of stripe (H_c^s) and bubble (H_c^b) domain coercivity on log of sample surface area S for sample A.

B. Size dependence of the anisotropy

The coercivity may be influenced by mechanical stresses in a magnetic body via the magnetoelastic interaction. The value of coercivity is proportional to local changes of the domain wall energy, and in this way, it is a function of local changes of the total anisotropy energy. In the epitaxial garnets the anisotropy is a combination of the cubic crystalline anisotropy K_1 , which can hardly be suspected to be size dependent, and the uniaxial anisotropy K_u , which, in turn, is composed of a growth-induced part K_u^g and a stress-induced part K_u^s . The main stresses in epitaxial garnets are due to the film-substrate lattice mismatch. However, this stress is independent of sample size, and it cannot be relaxed by sample cutting. Local changes of K_u^g and K_u^s around defects do not change with sample size either. No size dependence of the anisotropy has been experimentally measured. As a consequence, the measured coercivity changes can hardly be caused by a dependence of the anisotropy on the dimensions of the samples.

C. Effect of the paramagnetic substrate

Ferrimagnetic films can be grown on a paramagnetic $\text{Gd}_3\text{Ga}_5\text{O}_{12}$ substrate, with substantial susceptibility. We can estimate the contribution of its field-induced magnetization $4\pi M = \chi_s H_{\text{ext}}$ to the magnitude of the external field acting on the sample. The normal component of the magnetic induction inside the substrate, reduced by the demagnetizing field, is the same as the induction outside, but close to the surface it is given by

$$B_{\text{surf}} = H_{\text{ext}} + 4\pi M(1 - N_2). \quad (1)$$

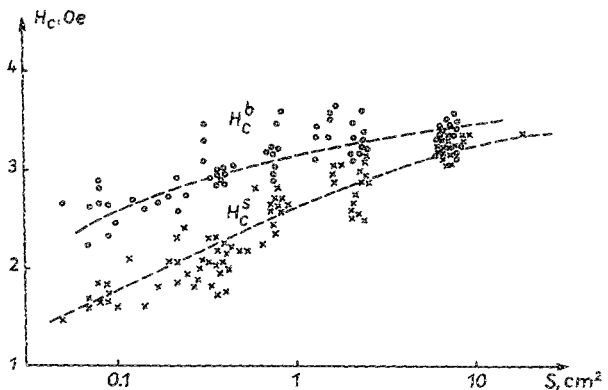


FIG. 4. Dependence of stripe (H_c^s) and bubble (H_c^b) domain coercivity on log of sample surface area S for sample B.

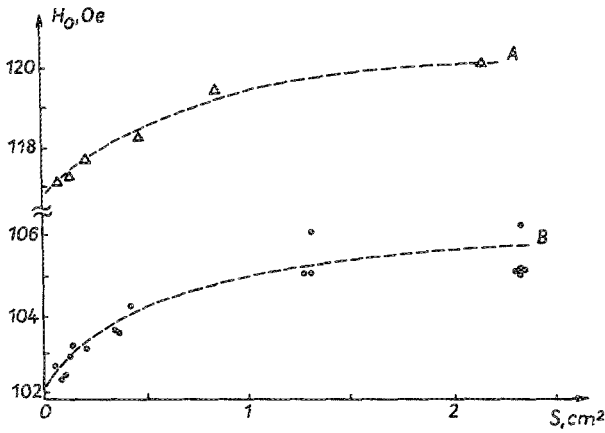


FIG. 5. Dependence of bubble domain collapse field H_0 on sample surface area S for samples A and B.

This means that the field acting on a film grown on a paramagnetic substrate with susceptibility χ_s and shape demagnetizing factor N_2 is

$$H_{\text{surf}} = H_{\text{ext}} [1 + \chi_s (1 - N_2)]. \quad (2)$$

For very large samples, $N \approx 1$ and $H_{\text{surf}} = H_{\text{ext}}$, but for the smallest sample used in the experiments, $(1 - N_2) \approx 0.3$. The measured susceptibility is $\chi_s \approx 0.0075$, and so the film feels a magnetic field larger by about 0.25% than the applied field H_{ext} . Because of this effect, the external field necessary to collapse the bubbles is smaller for smaller samples, but the

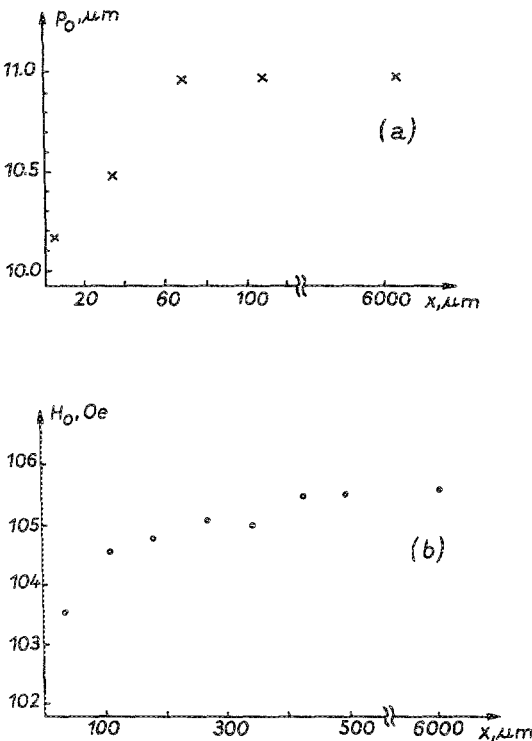


FIG. 6. Dependence of (a) p_0 stripe domain period and (b) H_0 bubble domain collapse field on distance x , measured from edge of sample. (Measurements were made on a 1.3-cm² piece of sample B.)

TABLE II. Stripe domain coercivity measured on a 9-cm² piece of sample B at different sites (a-e) of the sample. H_c^{s1} and H_c^{s2} denote the coercivity of domain structures, illustrated in Figs. 1 and 2, respectively.

	a	b	c	d	e
H_c^{s1} (Oe)	3.40	3.28	3.40	3.35	3.33
H_c^{s2} (Oe)	3.37	3.23	3.43	3.47	3.38

magnitude of this effect is about 10 times smaller than was observed experimentally.

D. Effect of sample boundaries and edges

The presence of sample boundaries influences the pattern of the domain structure, because, as a result of stray fields, the energy of any domain depends on its position relative to the sample boundaries. This influence was evaluated in Ref. 8 for a semi-infinite plate, and it was shown that the demagnetizing field is greatly reduced at the edges (by 50%), but this effect is limited to an area very near to the edges. At a distance of $5p_0$, the demagnetizing field reaches more than 90% of its "bulk" value inside the sample. In the present case the sample size is always much greater than the average domain size; even for the smallest sample, $S^{1/2} > 500p_0$. The boundary effect is able to reduce the domain size very near to the edge, but the size of the domains in the middle of the sample—where the measurements were carried out—was not changed. Consequently, the coercivity could not be affected by any change of the domain period due to the sample size, and in the areas of the actual measurement, such changes simply did not take place.

Some stripe domains are always pinned at the sample edges. In the large samples long stripes are pinned at the edges which are far from the area of measurement, and so the stripes can be influenced by this edge pinning in another way than shorter stripes in smaller samples where the edges are closer to the measuring point. However, bubbles and very short stripes (Fig. 2) are not pinned at the edges at all. In contrast to this the measured coercivities of the very short

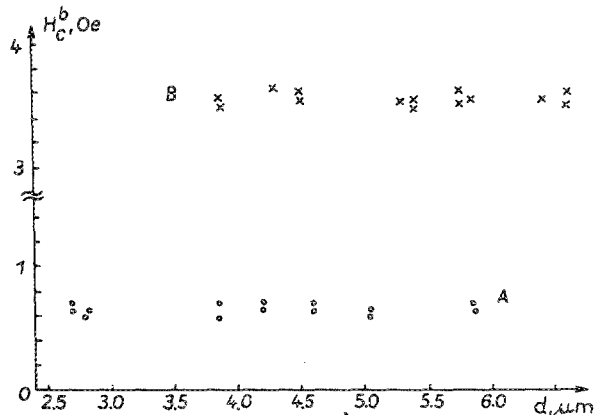


FIG. 7. Dependence of bubble domain coercivity (H_c^b) on bubble diameter d for samples A and B.

and long stripes in each sample are equal to one another and differ from that of bubbles. We conclude that the pinning of stripe domains at the edges of samples with different dimensions cannot be the reason for the sample size dependence of the measured coercivity. This conclusion is supported by the measurements, performed at various field distributions.

E. Domain geometry effects

The bubble array used for the measurement was a loose system of cylindrical domains with diameters substantially smaller than the mean bubble-to-bubble distance. In such a system the mutual interaction of neighbors is low, and in these limits the coercivity practically does not depend on the bubble diameter (see Fig. 7). What the coercivity does depend on, however, is the domain wall energy. The wall energy γ_w , listed in Table I, is the value calculated from the equilibrium stripe domain period and is valid for the long stripes of Fig. 1. The wall energy of the measured bubbles is probably different, because these bubbles were generated by the application of field pulses on the system of stripes, and as our samples were not ion implanted, the resulting array consisted mostly of hard bubbles, i.e., of bubbles with a considerable number of Bloch lines in their walls. As shown in Refs. 9 and 10, the coercivity measured on such a system of hard bubbles gives values increased by some 25% over those obtained on soft bubbles (e.g., on bubbles in ion-implanted samples or bubbles in any sample generated by a quasistatic large in-plane field).^{10,11} The generally larger absolute values of coercivity obtained for bubble domains as compared to stripes can partly be attributed to the larger wall energy density in the former system. The other part of the difference comes from the mutual interaction of neighboring domains.¹⁰

As the short stripes of Fig. 2 were obtained from the loose bubble array by a simple decrease of the bias field H_b down to zero, the same number of Bloch lines should exist in each short stripe as existed in each former bubble. However, the domain wall area of each short stripe is substantially larger than that of a bubble, so that the density of Bloch lines, and also the density of the wall energy, is considerably decreased. This fact, together with the observed clustering tendency of Bloch lines in oscillating walls,¹² explains why the coercivity measured on the short stripes is lower than that of the bubble array and practically equal to that of the long stripes.

F. Role of free-energy derivatives and change of the collapse field

The total free energy of a sample with domain structure is a function not only of the domain geometry and material parameters, but also of the sample shape and dimensions. The magnitude of the total energy per unit volume is actually not much influenced by the sample size—at least as long as the sample dimensions do not change in an extreme way—but the first and second derivatives of the total energy are very sensitive to sample size changes and so are all those physical parameters that directly depend on the energy de-

derivatives. The dependence of the bubble collapse field on the sample size can be interpreted in this way.

If we consider a circular sample with a finite diameter and a single bubble domain in the center of the sample, the bubble collapse field H_0 can be calculated according to Ref. 13 as

$$\frac{H_0}{4\pi M_s} = \frac{F(d_0/h) - l/h}{d_0/h}, \quad (3)$$

where d_0 is the collapse diameter of the bubble, and F is the Thiele bubble force function given by the first derivative of the sample total energy with respect to d . The bubble collapse diameter d_0 is the solution of the equation

$$S_0(d_0) = l/h, \quad (4)$$

where S_0 is the bubble radial stability function calculated from the first and second derivatives of the sample's total energy. In Ref. 13 the F and S_0 functions are presented for a single bubble in an *infinite* sample. In Ref. 14 the corresponding expressions of F and S_0 are given for a bubble in a *finite* plate.

The calculations of H_0 according to Ref. 14 and Eqs. (3) and (4) lead to a similar dependence of the collapse field in the sample size as observed. The calculated decrease of H_0 for our smallest sample is 1.1%, which is comparable to the measured value of 2.5%. Moreover, the *single* bubble approximation used for the calculation does not quite correspond to the experiment, which was performed on an array of *many* bubbles. To obtain still better agreement, the mutual interaction of bubbles [which influences the energy derivatives in a similar way as the limited sample size (see Ref. 15)] should be taken into account, too.

In principle, a change of the coercivity can cause a change of the measured value of the collapse field, because coercivity can influence the stability range of the bubble diameter d_0 and apparent measured H_0 . By application of a high-frequency ac field during the H_0 measurement (ac amplitude $\gg H_c$), the effect of coercivity can be avoided. This measurement proved that the sample size dependence of the bubble collapse field is an independent effect, not directly related to the size dependence of the measured coercivity.

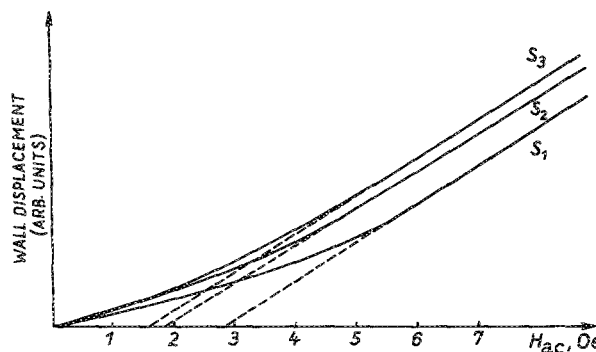


FIG. 8. Measured stripe domain coercivity curves for three pieces of sample B of differing size: $S_1 = 250 \text{ mm}^2$, $S_2 = 40 \text{ mm}^2$, and $S_3 = 5 \text{ mm}^2$.

G. Method of H_c measurement and the initial magnetization curve

The generally accepted measurement method¹ determines the domain wall coercivity H_c as the field amplitude extrapolated from the linear response of the domain wall motion versus the ac-field amplitude down to zero (illustrated in Fig. 8 for three different sample sizes). Each of the ac magnetization curves in Fig. 8 is composed of three typical parts. There is an initial linear part at very low field amplitudes, then comes a curved knee, and then again a linear part at higher fields. The initial linear part is understood as the region of fully reversible motion of domain walls. The walls are governed by the presence of the external field only to the extent that they do not leave their present local pinning coercive potential microwells. On the decrease of the field to zero, they return to the exact positions as before. There is no hysteresis for such small wall motions. Such a behavior of domain walls in the initial region of the field amplitudes has been confirmed experimentally.¹⁶ The higher field linear part of the curves in Fig. 8 corresponds to the irreversible motion of the domain walls when the applied field amplitude is high enough to move the domain walls without notice of the coercive potential microwells, and the shift of the straight line to the right in Fig. 8 gives the threshold field value H_c . The curved knee between the two linear parts corresponds to a transient state, i.e., to the average of the behavior of many domain walls in many coercive potential microwells in the area of measurement. Some walls start to move in the irreversible way sooner than the others; the spatial and strength distributions of the pinning points cannot be expected to be quite regular.

As seen from Fig. 8, it is the initial part of the curves that shortens and turns up if the sample size decreases. One of the mechanisms contributing to the shortening of the initial linear parts of the curves in Fig. 8 is the different shearing of the hysteresis loops as a consequence of the difference in the magnitude and the spatial distribution of the shape demagnetizing factor of the film itself in large and small samples. Because of the lower value of the demagnetization factor in a given external field, the domain walls of a small sample see a higher internal field than those of a large sample. As a consequence, in small samples a lower external field amplitude is strong enough to pull the walls beyond the initial coercive potential microwells. The initial linear parts of the curves (Fig. 8) are thus shortened, and we measure a lower H_c in small samples than in large ones. The change in the demagnetization factor of the magnetic film between our largest and smallest sample is only about 1%, and this cannot explain the effect quantitatively. Qualitatively, however, it can contribute to the observed dependence of the measured coercivity on the sample size.

The shortening of the initial linear part means that smaller field amplitudes are strong enough to overcome the maximum slope of the coercive potential microwells for domain wall motion. If the straight line starts to increase in a supralinear fashion, it means that the slope of the microwells is decreased, and the walls are moved by the field more easily, i.e., with higher susceptibility. Thus the smaller the sample, the shallower seem to be the initial coercive potential

microwells. In the same manner as was suggested in Ref. 17, we believe that this effect is mainly a consequence of the influence of the different steepness of the total free energy of the samples of different size, which adds up with the steepness of the true coercive potential microwells. Thus the general influence of the sample's total energy increases the pinning force of the local material fluctuations. In large samples the support is stronger, and in small ones the support is less strong. Here again, as in the case of the bubble-collapse-field calculation, the slope of total energy and sample initial susceptibility are expressed by the first and second energy derivatives, i.e., by quantities very sensitive to the sample dimensions.

The calculation of the total energy of a finite sample with a stripe domain structure is cumbersome because of the low symmetry of the problem. But it is not difficult to calculate the influence of the limited dimensions of the sample in the highly symmetrical case of a single bubble in a circular plate, and the calculation of the total energy as a function of the distance between bubble domains in a regular bubble array is rather easy. The susceptibility of bubble domains was calculated in Ref. 18, and the results qualitatively support the above arguments. A bubble surrounded by a closed system of neighboring bubbles (i.e., a cylindrical domain with magnetization $+4\pi M_s$ in the matrix domain having magnetization $-4\pi M_s$, partially surrounded by neighboring bubbles with magnetization $+4\pi M_s$) is qualitatively in a similar position to a bubble in a plate of a limited diameter (i.e., a cylindrical domain with magnetization $+4\pi M_s$ in the matrix domain having magnetization $-4\pi M_s$, completely surrounded by free space with zero magnetization). Thus the close-packed system of bubble domains can be considered as an approximate model system of a domain in a sample with limited dimensions. The properties of the total energy of an array of bubbles as a function of the decreased neighbor-to-neighbor distance should correspond to those of a bubble in a sample with decreasing dimensions (compare the corresponding curves in Ref. 15). Therefore, the coercivity measured on such a bubble array should decrease with the decrease of bubble-to-bubble distance, in full agreement with the experiment.¹⁰

V. CONCLUSIONS

It was observed experimentally that both stripe and bubble domain coercivity, measured by the wall oscillation method, significantly decrease with the decrease of the sample size from 2000 to 5 mm² of epitaxial garnet layers. The bubble collapse field was found to decrease by a few percent. Measurement of other parameters (stripe period, characteristic material length, domain wall energy, uniaxial anisotropy, saturation magnetization, and thickness) gave results that were independent of sample size.

Experiments showed that the change of domain wall length, of stress-induced anisotropy, the influence of domain pinning at the sample edges, or change of stripe domain period are not responsible for the observed sample size dependence of the measured coercivity and collapse field. The collapse field variations were found to be independent of those of the coercivity.

Three effects may jointly contribute to the observed sample size dependence of the measured coercivity. Two of them, the shearing of the hysteresis loop and the effect of the substrate demagnetization factor, modify the difference between the measured external applied field and internal field actually driving the domain walls. A quantitative estimate showed that both of these effects work in the proper direction, but they are both too weak to explain the measured values.

The third mechanism considered is the impact of the total free energy on the coercivity. In contrast to the first and second mechanisms, this third one changes the magnitude and range of the restoring force, since it changes the slope of the potential microwells. With suitably shaped intrinsic "material" microwells, even a very small change of the slope can cause an appreciable variation of the initial linear response in Fig. 8 and, therefore, of the wall coercivity measured according to Ref. 1. It has been shown that the first and second derivatives of the total free energy are sufficiently sensitive to the sample size to explain the observed effects. This effect has been directly demonstrated in the case of the collapse field changes.

In the case of the domain wall coercivity (which is measured and understood as the minimum field value necessary for the domain walls to start moving in an irreversible way), the full pinning force of the local potential microwells is assumed to be the sum of two effects: one being the true structural or material inhomogeneities that result in the distribution of the intrinsic potential microwells, the other being the total free energy of the whole sample which supports the steepness of the slope of the "material" microwells. This support is larger (greater dependence of the free energy of the sample on the position of the domain walls) in large samples and smaller in smaller ones, resulting in the observed sample

size dependence of coercivity. The assumption is in qualitative agreement with susceptibility calculations on samples with limited dimensions¹⁸ and was confirmed by a model experiment on an array of bubble domains in which the bubble-to-bubble distance was changed.¹⁰ A quantitative comparison with the theory is difficult without a more detailed knowledge of the actual shape of the intrinsic coercive potential microwells. Efforts are being made to obtain such information.

ACKNOWLEDGMENTS

The authors are grateful to G. J. Zimmer, P. Varga, and E. Kisdi-Koszó for their careful reading of the manuscript and valuable suggestions.

- ¹J. A. Seitchik, G. K. Goldberg, and W. D. Doyle, *J. Appl. Phys.* **42**, 1272 (1972).
- ²M. Balaskó and M. Pardavi-Horváth, *Appl. Phys.* **16**, 75 (1978).
- ³R. D. Henry, *IEEE Trans. Magn.* **MAG-13**, 1527 (1977).
- ⁴R. M. Josephs, *AIP Conf. Proc.* **10**, 286 (1972).
- ⁵H. Träuble, in *Moderne Probleme der Metallphysik*, edited by A. Seeger (Springer, Berlin, 1966), Vol. 2.
- ⁶H. Kronmüller, *J. Magn. Magn. Mater.* **24**, 159 (1981).
- ⁷H. R. Hilzinger and H. Kronmüller, *J. Magn. Magn. Mater.* **2**, 11 (1976).
- ⁸J. A. Cape and G. W. Lehmann, *J. Appl. Phys.* **42**, 5732 (1971).
- ⁹M. Pardavi-Horváth and G. Vértesy, *J. Appl. Phys.* **59**, 2113 (1986).
- ¹⁰G. Vértesy, L. Püst, and I. Tomáš, *J. Phys. D* **20**, 1088 (1987).
- ¹¹J. Kaczér and R. Gemperle, *Czech. J. Phys. B* **11**, 510 (1961).
- ¹²T. M. Morris, G. J. Zimmer, and F. B. Humphrey, *J. Appl. Phys.* **47**, 721 (1976).
- ¹³A. A. Thiele, *Bell Syst. Tech. J.* **48**, 3287 (1969).
- ¹⁴I. Tomáš and Z. Klem, *Phys. Status Solidi A* **42**, 459 (1977).
- ¹⁵I. Tomáš, *Phys. Status Solidi A* **21**, 329 (1974).
- ¹⁶I. Tomáš, G. Vértesy, and M. Balaskó, *J. Magn. Magn. Mater.* **42**, 287 (1984).
- ¹⁷I. Tomáš and G. Vértesy, *J. Magn. Magn. Mater.* **61**, 101 (1986).
- ¹⁸I. Tomáš, R. A. Szymczak, and J. Kaczér, *Phys. Status Solidi A* **16**, 439 (1973).